

# Journal of Mechanics of Materials and Structures

**PREDICTING THE EFFECTIVE STIFFNESS  
OF CELLULAR AND COMPOSITE MATERIALS  
WITH SELF-SIMILAR HIERARCHICAL MICROSTRUCTURES**

Yi Min Xie, Zhi Hao Zuo, Xiaodong Huang and Xiaoying Yang

Volume 8, No. 5-7

July–September 2013



# PREDICTING THE EFFECTIVE STIFFNESS OF CELLULAR AND COMPOSITE MATERIALS WITH SELF-SIMILAR HIERARCHICAL MICROSTRUCTURES

YI MIN XIE, ZHI HAO ZUO, XIAODONG HUANG AND XIAOYING YANG

Many natural and man-made materials exhibit self-similar hierarchical microstructures on several length scales. The effective macroscopic mechanical properties of such materials or composites are affected by the number of hierarchical levels and the topology of microstructures. Although the effective mechanical properties can be determined numerically using homogenization techniques, the computational costs can become prohibitively high as the level of hierarchy increases. This paper proposes an analytical approach to predicting the effective stiffness of a class of materials and structures with self-similar hierarchical microstructures. For each microstructural configuration, a simple relationship between the effective stiffness and the hierarchical level is established and verified against results of finite element analysis or data in the literature. It is found that the simple relationships we have developed provide quite accurate stiffness predictions of various hierarchical materials and composites including the Menger sponge. For composites, the predicted effective stiffness is accurate even when one of the phases is near its incompressibility limit, with its Poisson ratio close to 0.5. Inspired by the Menger sponge and informed by our topology optimization result, we propose a lighter yet stiffer “cross sponge”.

## 1. Introduction

Hierarchical solids contain structural elements which themselves have structures on more than one length scale [Lakes 1993]. Multilevel structural hierarchy, as observed in many living organisms, seems to be a universal strategy adopted by natural evolution for realizing remarkable properties and functions [Currey 1984; Aizenberg et al. 2005; Zhang et al. 2011].

According to Currey [1977; 1984] and Gao [2010], a sea shell has two to three levels of lamellar structure while bone has seven levels of structural hierarchy. It has been observed from many biological materials that the microstructures at different hierarchical levels often exhibit striking self-similarity [Jäger and Fratzl 2000; Puxkandl et al. 2002; Gao 2010; Zhang et al. 2011]. A mineralized tendon fiber, for example, has four levels of hierarchy with a highly ordered, self-similar structure at every level [Puxkandl et al. 2002; Zhang et al. 2011].

Among 3D solids with self-similar hierarchical structures or microstructures, the Menger sponge shown in Figure 1 is perhaps the most famous example. Starting from a solid cubic that is divided equally into  $3 \times 3 \times 3$  subcubes, the Menger sponge is created by simply removing the seven subcubes at the body and face centers of each remaining solid cube from the previous level. If the voids are replaced with an inclusion material, the Menger sponge becomes a composite with two phases. The Menger

---

This work is supported by the Australian Research Council's Discovery Projects (DP1094401).

*Keywords:* Menger sponge, cellular material, composite material, structural hierarchy, homogenization.

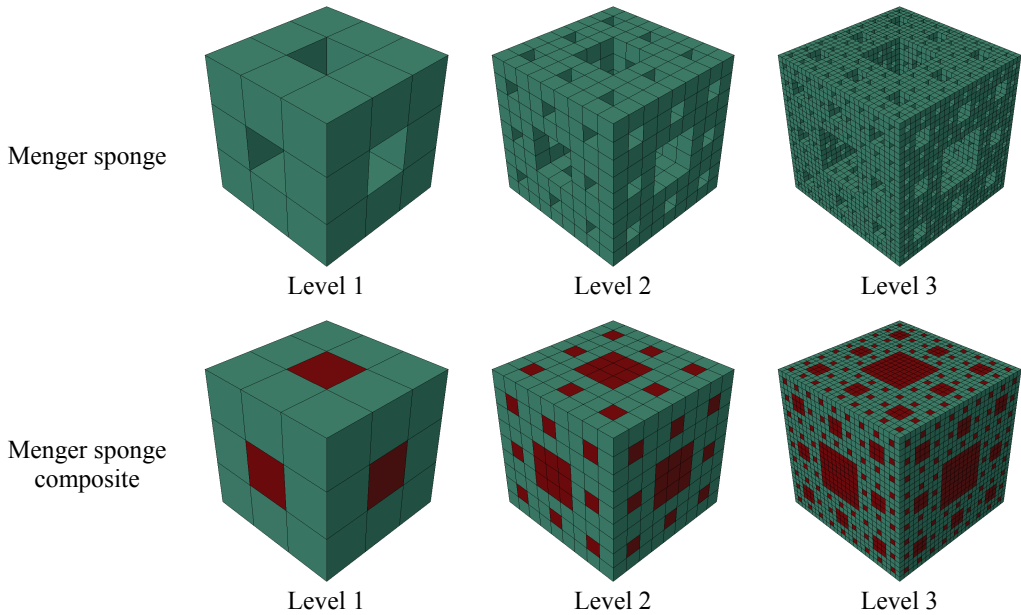


**Figure 1.** The first three levels of Menger sponges and Menger sponge composites.

sponge presents self-similar structural hierarchy since each subcube has the same topology as that of the cube of the previous level.

Figure 2 shows a level-three Menger sponge composite we have fabricated using the Connex350 3D printer [Stratasys 2012] which allows the simultaneous printing of two different materials. The transparent inclusion material is a rubber-like elastomer and the white matrix material is an acrylic-based glassy polymer.

There has been extensive research on the estimation of the macroscopic effective mechanical properties of load-carrying media [Watt et al. 1976; Sánchez-Palencia 1980; Coussy 1991; Tan et al. 1999; Liu et al. 2009]. For this purpose, numerical methods have been commonly applied; for instance, Hashin and Shtrikman [1962; 1963] proposed a variation approach for polycrystals and multiphase media, Cleary

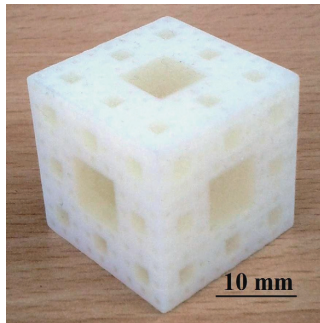


**Figure 2.** A level-three Menger sponge composite fabricated using a multimaterial 3D printer.

et al. [1980] used techniques of self-consistent approximations for heterogeneous media, Day et al. [1992] implemented a discretized-spring scheme for a sheet with circular inclusions, Garboczi and Day [1995] analyzed the mechanical properties of 3D composite using a finite element (FE) algorithm, and Poutet et al. [1996] applied a multiple-scale expansion scheme to random porous media including some hierarchical media. Apart from these, numerical homogenization techniques (for example, [Bakhvalov and Panasenko 1984; Nemat-Nasser and Hori 1993]) have been frequently used. Similarly, Steven [1997] and Tan et al. [2000] set up appropriate boundary conditions on a material base cell to attain elastic properties by using finite element analysis.

There has been limited work on the prediction of the effective physical and mechanical properties of hierarchical materials and structures. Thovert et al. [1990] studied the thermal conductivity of regular fractals and Poutet et al. [1996] examined elastic constants of a variety of porous media. However, due to the limitations of computer capacities of the time, only very low levels of the hierarchy were solved. This is because, as the level of hierarchy increases, computational cost can become prohibitively high. Oshmyan et al. [2001] studied the elastic properties of a special kind of self-similar hierarchical structures (2D Sierpinski-like structures) using FE-based simulations. They also considered Sierpinski composites with rigid inclusions. Our current work will cover general 3D self-similar hierarchical cellular structures as well as composites with deformable inclusions. Simple formulas for predicting the elastic moduli have been derived using the renormalization argument [Bergman and Kantor 1984; Poutet et al. 1996]. From the renormalization argument, Poutet et al. [1996] found that the ratio of the Young's moduli between two adjacent levels should be 2/3. Since then, this result has been accepted and cited by other researchers [Picu and Soare 2009]. We shall show in this paper that the prediction from the renormalization argument is inaccurate with an error of more than 20%. Indeed, even if one compares the numerical results of [Poutet et al. 1996] with the renormalization prediction, one can see differences of the same magnitude. In other words, the renormalization argument can be highly inaccurate. Therefore a new and more accurate approach to the prediction of the effective stiffness of self-similar hierarchical media needs be established. This will be the focus and the main contribution of the present paper. In addition, we shall propose a lighter yet stiffer hierarchical material than the Menger sponge.

## 2. Preliminary basics

**2.1. Terminology for mechanical properties.** In the literature, various terms are used to express the same item, such as the stiffness constitutive matrix, which can be denoted as a tensor  $\mathbf{C}$  or  $\mathbf{E}$ . The term stiffness may also refer to different mechanical quantities. For clarity, we shall first briefly define the terminology for mechanical properties. The following formula expresses Hooke's law in stiffness form with  $\mathbf{C}$  as the stiffness matrix:

$$\boldsymbol{\sigma} = \mathbf{C} \cdot \boldsymbol{\epsilon} \quad \text{or} \quad \begin{Bmatrix} \sigma_{11} \\ \sigma_{22} \\ \sigma_{33} \\ \sigma_{12} \\ \sigma_{23} \\ \sigma_{13} \end{Bmatrix} = \begin{bmatrix} C_{11} & C_{12} & C_{13} & C_{14} & C_{15} & C_{16} \\ C_{21} & C_{22} & C_{23} & C_{24} & C_{25} & C_{26} \\ C_{31} & C_{32} & C_{33} & C_{34} & C_{35} & C_{36} \\ C_{41} & C_{42} & C_{43} & C_{44} & C_{45} & C_{46} \\ C_{51} & C_{52} & C_{53} & C_{54} & C_{55} & C_{56} \\ C_{61} & C_{62} & C_{63} & C_{64} & C_{65} & C_{66} \end{bmatrix} \begin{Bmatrix} \epsilon_{11} \\ \epsilon_{22} \\ \epsilon_{33} \\ \epsilon_{12} \\ \epsilon_{23} \\ \epsilon_{13} \end{Bmatrix}. \quad (1)$$

Very often, Hooke’s law may be expressed using the engineering constants. Since the hierarchical media addressed in this paper are all symmetric with respect to the three middle planes, the orthotropic elasticity can be defined as

$$\begin{Bmatrix} \epsilon_{11} \\ \epsilon_{22} \\ \epsilon_{33} \\ \epsilon_{12} \\ \epsilon_{23} \\ \epsilon_{13} \end{Bmatrix} = \begin{bmatrix} 1/E_{11} & -\nu_{12}/E_{22} & -\nu_{13}/E_{33} & 0 & 0 & 0 \\ & 1/E_{22} & -\nu_{23}/E_{33} & 0 & 0 & 0 \\ & & 1/E_{33} & 0 & 0 & 0 \\ & & & 1/G_{12} & 0 & 0 \\ \text{Sym.} & & & & 1/G_{23} & 0 \\ & & & & & 1/G_{13} \end{bmatrix} \begin{Bmatrix} \sigma_{11} \\ \sigma_{22} \\ \sigma_{33} \\ \sigma_{12} \\ \sigma_{23} \\ \sigma_{13} \end{Bmatrix}, \tag{2}$$

where  $E_{11}$ ,  $E_{22}$ , and  $E_{33}$  denote the effective Young’s moduli in the three axial directions;  $\nu_{12}$ ,  $\nu_{23}$ , and  $\nu_{13}$  the Poisson’s ratios; and  $G_{12}$ ,  $G_{23}$ , and  $G_{13}$  the shear moduli. The stiffness discussed in this paper refers to the moduli  $E_{11}$ ,  $E_{22}$ , and  $E_{33}$ . Note that these moduli can also be calculated from the elastic constants as [Poutet et al. 1996]

$$E_{11} = C_{11} - \frac{2C_{12}^2}{C_{11} + C_{12}}. \tag{3}$$

Further, for a material with cubic symmetry, that is, with three mutually perpendicular symmetry planes ( $E_{11} = E_{22} = E_{33} = E$ ,  $\nu_{12} = \nu_{23} = \nu_{13} = \nu$ , and  $G_{12} = G_{23} = G_{13} = G$ ), such as the Menger sponge, the effective stiffness refers to the unique effective Young’s modulus  $E$ .

**2.2. Numerical homogenization through designed boundaries on unit cell.** A simple description of the numerical homogenization technique used in this study is presented here for 3D macroscopic mechanical characterization of an arbitrary structure or material microstructure. More details can be found in [Steven 1997; Tan et al. 2000].

The symmetry of the elastic stiffness matrix in (1) leaves 21 unknown constants to be determined. With six specified strain vectors, each with one strain component being unit and others being zero, we can calculate six elastic matrix constants easily. For example,

$$\begin{Bmatrix} \sigma_{11} \\ \sigma_{22} \\ \sigma_{33} \\ \sigma_{12} \\ \sigma_{23} \\ \sigma_{13} \end{Bmatrix} = \begin{Bmatrix} C_{11} \\ C_{21} \\ C_{31} \\ C_{41} \\ C_{51} \\ C_{61} \end{Bmatrix}, \quad \text{using the input strain } \epsilon^* = \begin{Bmatrix} \epsilon_{11} \\ \epsilon_{22} \\ \epsilon_{33} \\ \epsilon_{12} \\ \epsilon_{23} \\ \epsilon_{13} \end{Bmatrix} = \begin{Bmatrix} 1 \\ 0 \\ 0 \\ 0 \\ 0 \\ 0 \end{Bmatrix}. \tag{4}$$

In the numerical realization, six finite element analyses are required with unit strains expressed as prescribed displacements on the boundaries in order to get the corresponding stresses determined from the reaction forces. Two types of boundary conditions are involved: one with normal strain and the other with shear strain. Figure 3 demonstrates the two types of boundary conditions.

This simple and straightforward approach is capable of obtaining highly accurate results for the macroscopic mechanical properties of materials and structures, as suggested in [Steven 1997; Tan et al. 2000]. However, a sufficiently fine mesh is needed if the unit cell contains complex geometries such as arbitrary cavities or multiple phases. As an example, Figure 4 illustrates the effective stiffness obtained from

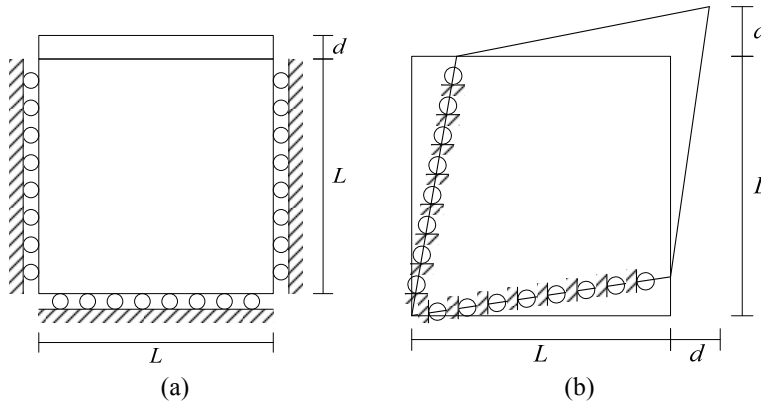


**Figure 3.** Boundary conditions used in the numerical homogenization: with (a) normal strain and (b) shear strain.

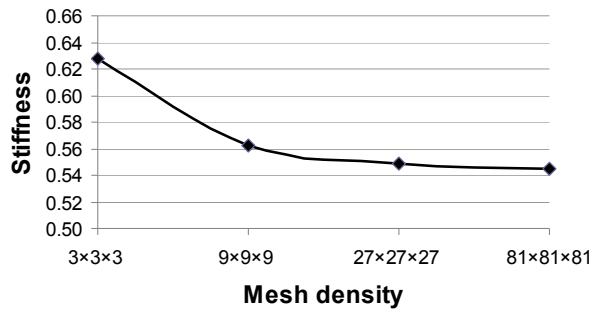


**Figure 4.** Numerical results of the stiffness of a level-one Menger sponge using different finite element meshes.

numerical homogenization using various finite element meshes. The chosen microstructure is the level-one Menger sponge shown in [Figure 1](#) with a base material of  $E_0 = 1$  and  $\nu = 0.2$ . The convergence of the stiffness results through mesh refinement is shown below. It is seen that even for the relatively simple shape of the level-one Menger sponge, a dense mesh (at least  $27 \times 27 \times 27$  or, to be more prudent,  $81 \times 81 \times 81$ ) should be used in order to obtain an accurate stiffness result.

### 3. Derivation of a stiffness prediction scheme

**3.1. The renormalization argument.** Several simplified models were presented in [[Poutet et al. 1996](#)] for stiffness predictions of various hierarchical media, including the Menger sponge. The basic idea of the renormalization argument is to decompose the Menger sponge into three homogeneous layers. Each layer's stiffness is simply assumed to be proportional to the cross-sectional area. The stiffness for the whole sponge can then be calculated through a simple force and deformation relationship. However, the prediction failed to match with the numerical results, in which the stiffness ratio between two adjacent levels ranged from 0.53 to 0.58, significantly different from the renormalization prediction of  $2/3$ .

If we look carefully at the simplified model of the Menger sponge within the renormalization argument, we will find that the force from one face to the opposite face is not transmitted evenly through the three layers, that is, stress concentrations will be found at the actual connections between layers. In this sense, the simplified model overestimates the effective stiffness.

**3.2. Stiffness prediction through a bounded estimation scheme.** Due to the nonuniform geometry, it is difficult or inaccurate to use only one simplified model to describe the force and deformation relationship of a hierarchical material such as the Menger sponge. However, one may set up multiple simplified models to predict the real value within a certain range. In this vein, we propose a scheme to calculate the stiffness based on the under and overestimates.

As an example, the Menger sponge can be simplified in two different ways, as shown in Figure 5. In the first model, eight white-colored blocks in the top and bottom layers are ignored, as shown in Figure 5(a). This is based on the assumption that under vertical pressure loading on the top and bottom surfaces these eight blocks are only weakly stressed. In this case, the Menger sponge is simplified and transformed into a parallel connection of four columns in the force direction. Since this parallel decomposition ignores the existence of the removed parts and thus ignores their stiffness, this simplified model underestimates the actual stiffness of the Menger sponge. The underestimate of stiffness is approximated as proportional to the cross-sectional area. Note that each constitutive block of a level- $n$  Menger sponge is a level- $(n - 1)$  Menger sponge due to the self-similarity, and that the stiffness of a full cube model with all such blocks is naturally equal to the stiffness of a level- $(n - 1)$  Menger sponge. Since four out of the nine columns of the full cube model are left, the stiffness of a level- $n$  Menger sponge can be simply determined as  $4/9$  of that of the level- $(n - 1)$  Menger sponge. In (5) the subscript denotes the level and the superscript

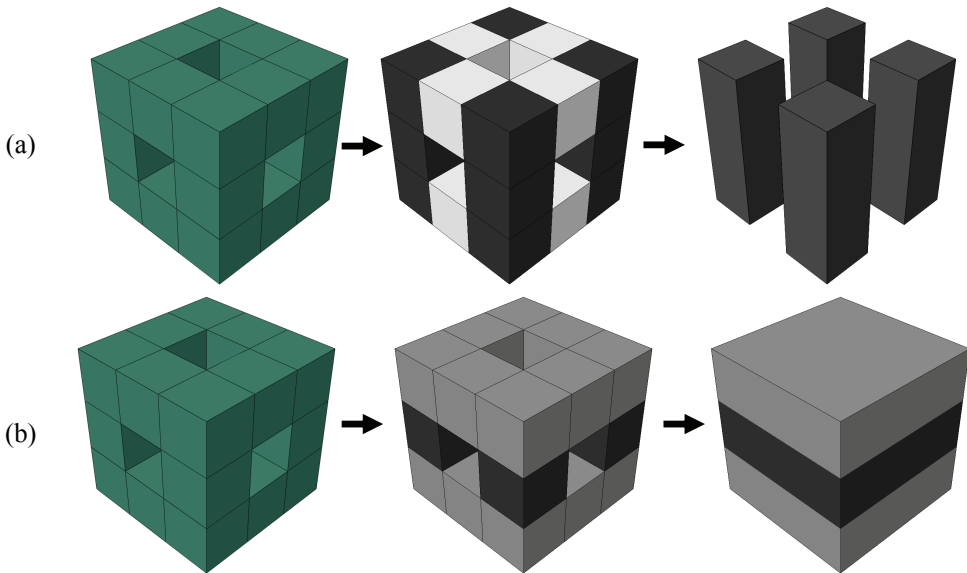


**Figure 5.** Simplified models of the level-one Menger sponge: (a) parallel connection model and (b) serial-connection model.

denotes the underestimate:

$$E_n^- = \frac{4E_{n-1}}{9}. \quad (5)$$

The aforementioned renormalization argument is referred to for the second model, which consists of three homogenized layers. This decomposition using serial connections, as in [Figure 5\(b\)](#), overestimates the stiffness as mentioned earlier and as supported by the numerical results from [[Poutet et al. 1996](#)]. The effective Young's moduli of each layer can be simplified as  $8E_{n-1}/9$ ,  $4E_{n-1}/9$ , and  $8E_{n-1}/9$ , respectively. With  $p$  being the pressure acting on the top and bottom faces of the Menger sponge, and  $a$  being the thickness of each layer, the normal strain is calculated as

$$\begin{aligned} \epsilon_{xx} &= \frac{p}{E_n} = \frac{d_{xx}}{3a} = \frac{1}{3} \left( \frac{d_{xx,1} + d_{xx,2} + d_{xx,3}}{a} \right) = \frac{1}{3} (\epsilon_{xx,1} + \epsilon_{xx,2} + \epsilon_{xx,3}) \\ &= \frac{1}{3} \left( \frac{p}{8E_{n-1}/9} + \frac{p}{4E_{n-1}/9} + \frac{p}{8E_{n-1}/9} \right), \end{aligned} \quad (6)$$

where the second subscript in the displacement and strain denotes the layer number. Hence we obtain the effective stiffness of the overestimation model as

$$E_n^+ = \frac{2E_{n-1}}{3}. \quad (7)$$

The Reuss [[1929](#)] bound and the Voigt [[1889](#)] bound have been believed to be the lower and upper bounds of the effective stiffness of composites. These two bounds correspond to the serial and parallel-connection models, respectively, which seems contrary to the proposal in this paper. However, being different from the Reuss and Voigt models, the model decomposition in this paper is valid also for cellular hierarchical materials, and building blocks are deliberately removed or added to form a weaker or stronger simplified model for analytical calculation of the stiffness. As a result, artificial upper and lower estimates are obtained that actually work as the bounds for the effective stiffness.

The overestimated stiffness is obviously larger than the underestimated stiffness. The real value of the stiffness is deemed to lie between the above under and overestimates. Hence we can set up the following framework for an effective approximation using an interpolation scheme:

$$E_n = (1 - \alpha)E_n^- + \alpha E_n^+, \quad \text{with } 0 \leq \alpha \leq 1, \quad (8)$$

and particularly for the Menger sponge:

$$E_n = \frac{2}{3}\alpha E_{n-1} + \frac{4}{9}(1 - \alpha)E_{n-1} = \frac{4+2\alpha}{9} E_{n-1}. \quad (9)$$

The interpolation parameter  $\alpha$  in the above formula applies to all levels of the hierarchy in theory. Therefore  $\alpha$  can be simply calculated by substituting the stiffnesses of levels-zero and one Menger sponges. A level-zero Menger sponge refers to the solid, isotropic base material. The stiffness of the level-one Menger sponge is obtained numerically using the numerical homogenization approach introduced in [Section 2](#). Due to the cavities in the level-one Menger sponge, a very fine finite element mesh  $3^4 \times 3^4 \times 3^4$  is used in finite element analysis (FEA) to get accurate results, as mentioned earlier. With  $E_0 = 1$  and  $\nu_0 = 0.2$ , the FEA result gives  $E_1 = 0.5450$ . From (9),  $\alpha$  is obtained as 0.4525. Therefore, the stiffness



Level	Numerical	$E_n^-$	$E_n^+$	Predicted	Difference	[Poutet et al. 1996]	RA
1	0.5450	0.4444	0.6666	0.5450	0.00%	0.53298	0.6666
2	0.3077	0.1975	0.4444	0.2970	3.48%	0.29771	0.4444
3	0.1718	0.0878	0.2963	0.1619	5.76%	0.1737	0.2963
4	0.0960	0.0390	0.1975	0.0882	8.13%	N/A	0.1975

**Table 1.** Summary of stiffnesses of Menger sponges of different levels, with  $E_0 = 1$  and  $\nu_0 = 0.2$ .

prediction formula is further simplified as

$$E_n = 0.5450E_{n-1} \quad \text{or} \quad E_n = 0.5450^n E_0. \tag{10}$$

In order to examine the accuracy of the proposed prediction of effective stiffness, further levels of the Menger sponge have been solved using numerical homogenization. The numerical results are summarized in Table 1 with comparison to the under and overestimated stiffnesses, the predicted stiffness values using (10), the numerical results of [Poutet et al. 1996], and the predictions of the renormalization argument (RA).

Through the hierarchical level increasing, the stiffness under and overestimates differ more and more from the numerical results due to the built-up errors caused by the model simplifications. Nevertheless, the bounds give a practical estimate of the effective stiffness before any accurate homogenization technique is applied. The renormalization argument actually gives an upper bound of the effective stiffness. The predicted effective stiffnesses match well with the numerical results, and with the previous numerical results of [Poutet et al. 1996]. In contrast, the renormalization argument gives values that are at least 20% different from the numerical results. Due to limited computer power in the 1990s, Poutet et al. [1996] only solved the first three levels of the Menger sponge. In our study, the meshes we have used for levels-one to three Menger sponges are  $3^4 \times 3^4 \times 3^4$ ,  $3^4 \times 3^4 \times 3^4$ , and  $3^5 \times 3^5 \times 3^5$ , respectively. Since the Menger sponge is cubic symmetric, a one-eighth model is used for level four with a  $(2 \times 3^5) \times (2 \times 3^5) \times (2 \times 3^5)$  mesh to balance the numerical accuracy and computational cost. Note that due to voids in the Menger sponges, the actual numbers of solid elements in the above four meshes are  $3^4 \times 3^4 \times 3^4 \times 20/27$ ,  $3^4 \times 3^4 \times 3^4 \times (20/27)^2$ ,  $3^5 \times 3^5 \times 3^5 \times (20/27)^3$ , and  $(2 \times 3^5) \times (2 \times 3^5) \times (2 \times 3^5) \times (20/27)^4$ . It is seen that the basic building block — a unit structure with a level-one Menger sponge pattern — is much more coarsely meshed in the level-four Menger sponge than in the level-one Menger sponge. In other words, an extremely fine mesh,  $3^7 \times 3^7 \times 3^7$ , should be used for level four in order to achieve an equal numerical accuracy to level one. However even a supercomputer would have difficulty in handling such a fine mesh. Nevertheless, if such a fine mesh is achieved, the numerical stiffness is expected to decrease as indicated in Figure 4. In this case, it is envisaged that the numerical results will match the predicted values even better.

#### 4. Stiffness prediction for hierarchical composites

Stiffness of hierarchical composites can be predicted in the same way as for hierarchical media of a single base material as discussed in Section 3. Taking the Menger sponge composite in Figure 6 for example,

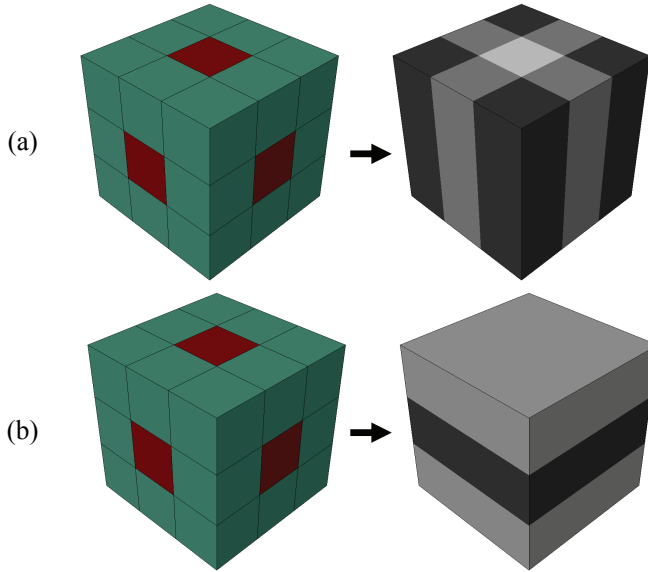


**Figure 6.** Simplified models for a Menger sponge composite of level one: (a) parallel-connection model and (b) serial-connection model.

two simplified models are similarly introduced for stiffness estimates. The composite is assumed to have two base materials, with  $E_m$  being the Young's modulus for the matrix base material (green) and  $E_i$  for the inclusion material (red). Note that a level- $n$  Menger sponge composite of stiffness  $E_n$  consists of 20 blocks of level- $(n - 1)$  Menger sponge composite of  $E_{n-1}$  and seven blocks of pure inclusion base material of  $E_i$ .

The first simplified model decomposes the level- $n$  Menger sponge composite into nine parallel columns. The Young's moduli for the four corner columns and the central column are  $E_{n-1}$  and  $E_i$ , respectively, while the Young's modulus of the remaining four columns is estimated by a simple force and deformation relationship. Suppose a pressure  $p$  is applied on one of these four columns that is composed of three blocks with Young's moduli  $E_{n-1}$ ,  $E_i$ , and  $E_{n-1}$ , respectively, the strain will be calculated as  $(p/E_{n-1} + p/E_i + p/E_{n-1})/3$ . On the other hand, the strain can also be calculated as the pressure divided by the homogenized Young's modulus of the whole column. Therefore the effective Young's modulus for these columns can be obtained based on a simple calculation and given as  $3E_{n-1}E_i/(E_{n-1} + 2E_i)$ . Finally, we have the first estimate of the effective stiffness of the whole composite as

$$E_n^- = \frac{1}{9} \left( 4E_{n-1} + E_i + 12 \frac{E_{n-1}E_i}{E_{n-1} + 2E_i} \right). \quad (11)$$

Similarly as in the single base material case, the second simplified model decomposes a level- $n$  Menger sponge composite into three serial-connected homogenized layers. With a simplification of stiffness proportional to the cross-sectional areas, the estimated Young's moduli for the three layers are  $8E_{n-1}/9 + E_i/9$ ,  $4E_{n-1}/9 + 5E_i/9$ , and  $8E_{n-1}/9 + E_i/9$ , respectively. With  $p$  being the pressure applied to the top and bottom faces of the composite, the total deformation in the force direction is calculated similarly as

Level	Numerical	$E_n^-$	$E_n^+$	Predicted	Difference
1	0.5647	0.4586	0.6712	0.5647	0.00%
2	0.3311	0.2177	0.4520	0.3228	2.51%
3	0.2000	0.1101	0.3059	0.1884	5.80%

**Table 2.** Summary of stiffnesses of Menger sponge composites with  $E_0 = 1$ ,  $\nu_0 = 0.2$ ,  $E_i = 0.01$ , and  $\nu_i = 0.4$ .

Numerical	Predicted	Difference
$4.3616 \times 10^{10}$	$4.3616 \times 10^{10}$	0.00%
$2.7862 \times 10^{10}$	$2.7428 \times 10^{10}$	1.56%
$1.8235 \times 10^{10}$	$1.7490 \times 10^{10}$	4.09%

**Table 3.** Summary of stiffnesses of Menger sponge composites with  $E_0 = 70 \times 10^9$ ,  $\nu_0 = 0.33$ ,  $E_i = 1 \times 10^9$ , and  $\nu_i = 0.49$ .

in (6):

$$\epsilon_{xx} = \frac{p}{E_n} = \frac{1}{3} \left( \frac{p}{8E_{n-1}/9 + E_i/9} + \frac{p}{4E_{n-1}/9 + 5E_i/9} + \frac{p}{8E_{n-1}/9 + E_i/9} \right). \tag{12}$$

Hence we obtain the second estimated stiffness as

$$E_n^+ = \frac{32E_{n-1}^2 + 44E_{n-1}E_i + 5E_i^2}{48E_{n-1} + 33E_i}. \tag{13}$$

Within the framework established by (8), we get the stiffness prediction

$$E_n = \frac{1}{9}(1 - \alpha) \left( 4E_{n-1} + E_i + 12 \frac{E_{n-1}E_i}{E_{n-1} + 2E_i} \right) + \alpha \frac{32E_{n-1}^2 + 44E_{n-1}E_i + 5E_i^2}{48E_{n-1} + 33E_i}. \tag{14}$$

It is worth pointing out that the Menger sponge is a special case of the Menger sponge composite. If the inclusion base material is replaced with void, that is,  $E_i = 0$ , the stiffness prediction in (14) reduces to that in (9).

The parameter  $\alpha$  is determined by the stiffnesses of levels-zero and one Menger sponge composites, where accurate results can be obtained with feasible fine meshes. In fact, no computation is required for level zero as it refers to the solid matrix base material. In the first case, it is assumed that the matrix base material has  $E_0 = 1$  and  $\nu_0 = 0.2$ , and the inclusion base material has  $E_i = 0.01$  and  $\nu_i = 0.4$ . The FEA result gives  $E_1 = 0.5647$ . From (14),  $\alpha$  is obtained as 0.4987. Table 2 presents the stiffnesses of various Menger sponge composites composed of these two base materials, with comparison between the numerical values and the predicted stiffnesses from (14). Meshes of  $3^3 \times 3^3 \times 3^3$ ,  $3^4 \times 3^4 \times 3^4$ , and  $3^5 \times 3^5 \times 3^5$  are used for levels one to three, respectively. In another case, the composite is assumed to have aluminum as the matrix base material, with  $E_0 = 70 \times 10^9$  and  $\nu_0 = 0.33$ , and silicon rubber as the inclusion base material, with  $E_i = 1 \times 10^9$  and  $\nu_i = 0.49$ . For the latter case,  $\alpha$  is obtained as 0.7599 and the results summary is given in Table 3.

More computational effort is needed for composites than for single-base material media because the finite element model is always a full model without any voids. Therefore only the first three levels of the Menger sponge composites are solved. Again through the hierarchical level increasing, the stiffness under and overestimates expand to make a wider and wider range into which the numerical result falls. The predicted stiffness values match well with the numerical results, even when the inclusion base material is almost incompressible, with its Poisson's ratio close to 0.5. This finding is of special importance because when one of the phases of the composite is near its incompressibility limit, it is usually necessary to use a different and more sophisticated analytical model in order to predict the effective stiffness accurately [Liu et al. 2006; 2009]. However, our proposed simple formula in (14) does not have this problem.

### 5. Stiffness prediction for a different self-similar hierarchical medium

Similar to the Menger sponge, whose basic topology can be defined based on a cube divided into  $3 \times 3 \times 3$  blocks, various other self-similar hierarchical media can be created by specifying different recursive rules for block removal. We propose an alternative hierarchical "sponge" that is obtained by removing eight corner blocks as well as the central one, as shown in Figure 7. Since this hollow material presents a cross shape in all three faces, we name it the "hollow cross sponge". The base material is selected as  $E_0 = 1$  and  $\nu_0 = 0.2$ .

To predict the stiffness of such a hierarchical material, two simplified models in Figure 8 with parallel and serial connections are employed, as we have done with the Menger sponge.

In the first simplified model, the whole structure is decomposed into four columns since the other parts form no direct connection in the axial force direction. The parts removed make the simplified model underestimate the actual stiffness. Similarly as in the case described in (5), four out of nine columns of the full-cube model are left and the stiffness of this underestimation model is easily determined based on the cross-sectional area:

$$E_n^- = \frac{4E_{n-1}}{9}. \quad (15)$$

For the serial-connection model, the Young's moduli of the three homogenized layers are estimated as  $5E_{n-1}/9$ ,  $8E_{n-1}/9$ , and  $5E_{n-1}/9$ , respectively, based on the areas. In a simple derivation of the force and deformation relationship as in (6), the overestimated stiffness of the whole sponge is found as

$$E_n^+ = \frac{40E_{n-1}}{63}. \quad (16)$$

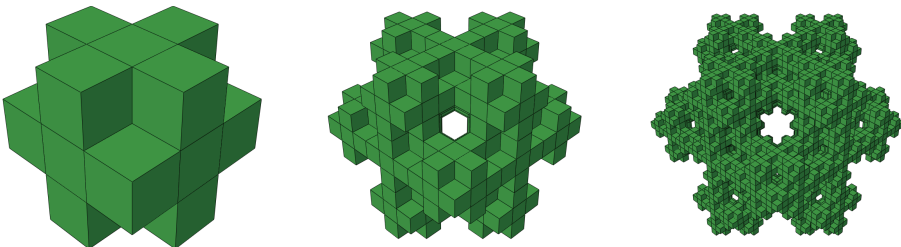


**Figure 7.** The first three levels of an alternative hierarchical material: the hollow cross sponge.

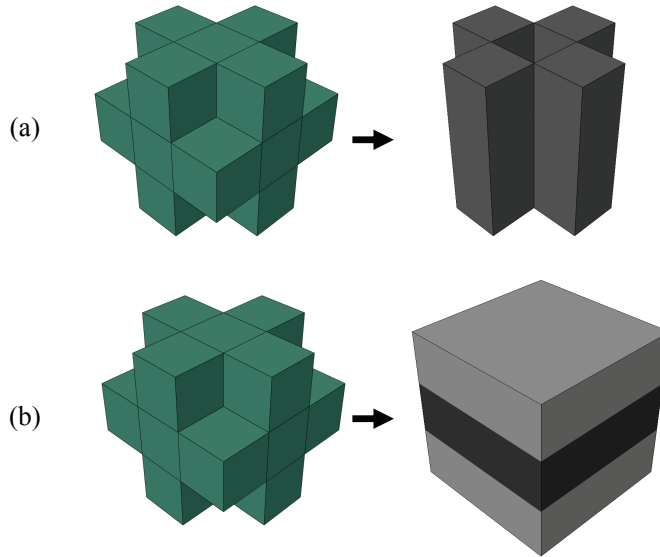


**Figure 8.** Simplified models of the hollow cross sponge, with all eight corner blocks and the central block removed: (a) parallel-connection model and (b) serial-connection model.

In the framework set up in (8), the effective stiffness of the sponge is predicted as

$$E_n = \frac{4}{9}(1 - \alpha)E_{n-1} + \frac{40}{63}\alpha E_{n-1} = \frac{28+12\alpha}{63}E_{n-1}. \tag{17}$$

Assume that the base material has  $E_0 = 1$  and  $\nu_0 = 0.2$ . The parameter  $\alpha$  can be determined from  $E_1$ , which is found to be equal to 0.5087 from the numerical homogenization applied to the level-one sponge in Figure 7. This results in  $\alpha = 0.3373$ . Table 4 shows the stiffnesses of various levels of the hollow cross sponge using  $E_0 = 1$  and  $\nu_0 = 0.2$  for the purpose of examining the accuracy of the predicted effective stiffness. It is seen that the under and overestimates give effective bounds for the effective stiffness, and that the predictions from the simple formula in (17) are reasonably accurate.

### 6. Proposing a lighter yet stiffer material than the Menger sponge

The stiffness of a hierarchical medium depends on the topology and the amount of base material. To find a design with a higher stiffness for a predefined amount of material usage, topology optimization techniques can be employed. Figure 9 shows an optimal material base cell for maximizing the effective

Level	Numerical	$E_n^-$	$E_n^+$	Predicted	Difference
1	0.5087	0.4444	0.6349	0.5087	0.00%
2	0.2538	0.1975	0.4031	0.2588	1.98%
3	0.1253	0.0878	0.2560	0.1316	5.05%
4	0.0617	0.0390	0.1625	0.0670	8.63%

**Table 4.** Summary of stiffnesses of the first four levels of the hollow cross sponge.

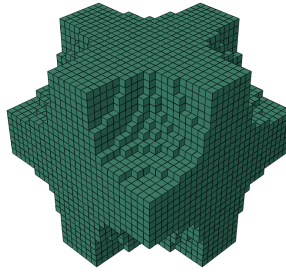


**Figure 9.** Optimal topology for maximizing the effective stiffness for a given amount of volume.

stiffness we have obtained using the ESO/BESO topology optimization technique [Xie and Steven 1993; 1997; Huang and Xie 2007; 2010; Yang et al. 2013]. The optimization is based on the volume fraction of  $19/27$  and the cubic symmetric constraint, that is, the effective stiffnesses in the three directions are set equal to each other. The elastic properties of the base material are  $E_0 = 1$  and  $\nu_0 = 0.2$ . The effective stiffness of this design is 0.5864.

Informed by the above optimal topology, we propose to construct a new sponge as shown in Figure 10. Starting from a cube with  $3 \times 3 \times 3$  blocks, we remove the eight corner blocks. This will create a design of a similar topology to, and with the same volume as, the optimal solution shown in Figure 9. Since this model presents a cross in a 2D view from all three faces, we name it the “cross sponge”. From this basic configuration, we can recursively create a series of self-similar sponges of any level.

The under and overestimates of the cross sponge stiffness can be derived from the two simplified models shown in Figure 11:

$$E_n^- = \frac{5E_{n-1}}{9}, \tag{18}$$

$$E_n^+ = \frac{15E_{n-1}}{23}, \tag{19}$$

and the stiffness prediction formula is defined as

$$E_n = \frac{5}{9}(1 - \alpha)E_{n-1} + \frac{15}{23}\alpha E_{n-1} = \frac{115+20\alpha}{207}E_{n-1}. \tag{20}$$

The parameter  $\alpha$  is then determined from the level-zero (assuming  $E_0 = 1$  and  $\nu_0 = 0.2$ ) and level-one sponges ( $E_1 = 0.5816$  from numerical results). This results in  $\alpha = 0.2696$ . The stiffness of the cross

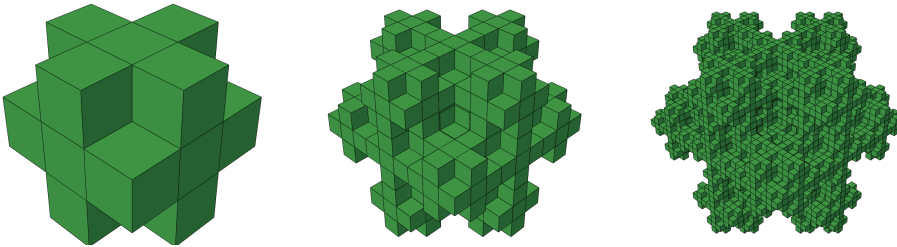


**Figure 10.** The proposed cross sponge, which is lighter yet stiffer than the Menger sponge.

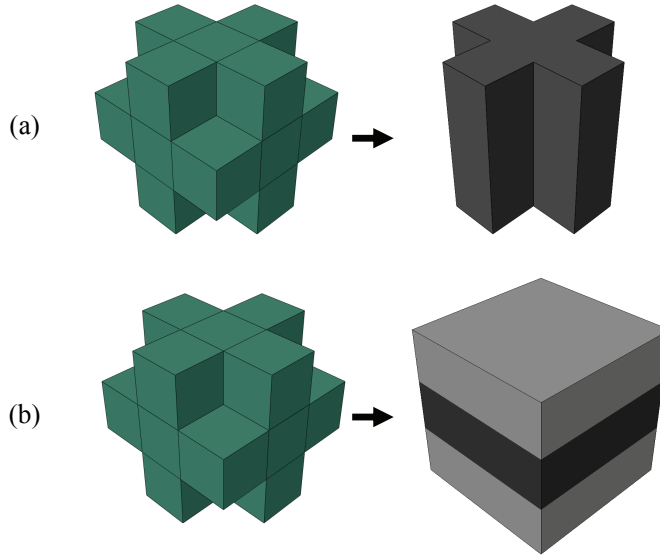


**Figure 11.** Simplified models of the cross sponge: (a) parallel-connection model and (b) serial-connection model.

Level	Numerical	$E_n^-$	$E_n^+$	Predicted	Difference
1	0.5816	0.5556	0.6522	0.5816	0.00%
2	0.3321	0.3086	0.4253	0.3383	1.87%
3	0.1914	0.1715	0.2774	0.1967	2.77%
4	0.1085	0.0953	0.1809	0.1144	5.44%

**Table 5.** Summary of stiffnesses of the first four levels of the cross sponge.

sponge is higher than that of the Menger sponge (0.5816 versus 0.5450) even though the cross sponge is lighter (19/27 versus 20/27). [Table 5](#) compares the stiffnesses of various levels of the cross sponge. It is seen that the predicted stiffnesses using the simple formula in [\(20\)](#) are quite accurate.

## 7. Concluding remarks

This paper has presented an analytical approach for stiffness prediction of hierarchical media. Unlike the previous renormalization argument, which uses only one simplified model and thus yields highly inaccurate stiffness predictions, the proposed approach employs two simplified models that under and overestimate the effective stiffness. The predicted stiffness is calculated as an interpolation between the under and overestimates. As the prediction presents the relationship between the stiffness of two adjacent levels, the interpolation parameter is determined based on the two lowest levels for which accurate numerical values can be easily obtained. The proposed approach for stiffness prediction is applicable to a whole class of self-similar hierarchical media, including composites, as demonstrated by a range of examples in this paper. The simple formulas developed have been found to give accurate predictions of stiffnesses of self-similar hierarchical media of various levels. For composites, the predicted effective

stiffness is accurate even when one of the phases is near its incompressibility limit, with its Poisson's ratio close to 0.5.

Inspired by the Menger sponge and informed by our topology optimization result, we have proposed a lighter yet stiffer cross sponge.

It is interesting to note that Lakes [1993] predicted that the effective stiffness of hierarchical materials should follow the relationship

$$\frac{E_n}{E_0} = k^n \left[ \frac{\rho_n}{\rho_0} \right]^r, \quad (21)$$

where  $k$  and  $r$  are coefficients depending on the type of structure,  $\rho$  is the density, and  $\rho_0$  is the density of the solid phase. If we look at (9), (17), and (20), we will find that the proposed stiffness prediction formulas agree with Lakes' assumption, given in (21). Take the Menger sponge as an example. The mass density can be calculated as

$$\rho_n = \left( \frac{20}{27} \right)^n \rho_0. \quad (22)$$

Thus (10) may be transformed into the same format as that of Lakes' formula if we assign  $r = 1$  and  $k = 0.7358$ :

$$\frac{E_n}{E_0} = 0.7358^n \left[ \frac{\rho_n}{\rho_0} \right] = 0.5450^n. \quad (23)$$

In fact, according to the proposed scheme based on the simplified models in this paper, the stiffness prediction for hierarchical media with one base material can be generalized into

$$\frac{E_n}{E_0} = \beta^n, \quad (24)$$

where  $\beta$  is a constant. One can determine the  $\beta$  value to make the prediction explicit; on the other hand, one may also use the effective stiffnesses of the simplified models proposed in this paper as bounds for a rough estimation.

## References

- [Aizenberg et al. 2005] J. Aizenberg, J. C. Weaver, M. S. Thanawala, V. C. Sundar, D. E. Morse, and P. Fratzl, "Skeleton of *Euplectella* sp.: structural hierarchy from the nanoscale to the macroscale", *Science* **309**:5732 (2005), 275–278.
- [Bakhvalov and Panasenko 1984] N. Bakhvalov and G. Panasenko, *Осреднение процессов в периодических средах*, Nauka, Moscow, 1984. Translated as *Homogenisation: averaging processes in periodic media*, Mathematics and its Applications (Soviet Series) **36**, Kluwer Academic, Dordrecht, 1989.
- [Bergman and Kantor 1984] D. J. Bergman and Y. Kantor, "Critical properties of an elastic fractal", *Phys. Rev. Lett.* **53**:6 (1984), 511–514.
- [Cleary et al. 1980] M. P. Cleary, S.-M. Lee, and I.-W. Chen, "Self-consistent techniques for heterogeneous media", *J. Eng. Mech. (ASCE)* **106** (1980), 861–887.
- [Coussy 1991] O. Coussy, *Mécanique des milieux poreux*, Editions Technip, Paris, 1991.
- [Currey 1977] J. D. Currey, "Mechanical properties of mother of pearl in tension", *Proc. R. Soc. Lond. B* **196** (1977), 443–463.
- [Currey 1984] J. D. Currey, *The mechanical adaptations of bones*, Princeton University Press, 1984.
- [Day et al. 1992] A. R. Day, K. A. Snyder, E. J. Garboczi, and M. F. Thorpe, "The elastic moduli of a sheet containing circular holes", *J. Mech. Phys. Solids* **40** (1992), 1031–1051.



- [Gao 2010] H. Gao, “Learning from nature about principles of hierarchical materials”, pp. 65–68 in *Proceedings of the 3rd International Nanoelectronics Conference* (Hong Kong, 2010), edited by P. K. Chu, IEEE, Piscataway, NJ, 2010.
- [Garboczi and Day 1995] E. J. Garboczi and A. R. Day, “An algorithm for computing the effective linear elastic properties of heterogeneous materials: 3-D results for composites with equal phase Poisson ratios”, *J. Mech. Phys. Solids* **43**:9 (1995), 1349–1362.
- [Hashin and Shtrikman 1962] Z. Hashin and S. Shtrikman, “A variational approach to the theory of the elastic behaviour of polycrystals”, *J. Mech. Phys. Solids* **10** (1962), 343–352.
- [Hashin and Shtrikman 1963] Z. Hashin and S. Shtrikman, “A variational approach to the theory of the elastic behaviour of multiphase materials”, *J. Mech. Phys. Solids* **11** (1963), 127–140.
- [Huang and Xie 2007] X. Huang and Y. M. Xie, “Convergent and mesh-independent solutions for the bi-directional evolutionary structural optimization method”, *Finite Elem. Anal. Des.* **43**:14 (2007), 1039–1049.
- [Huang and Xie 2010] X. Huang and Y. M. Xie, *Evolutionary topology optimization of continuum structures: methods and applications*, Wiley, Chichester, 2010.
- [Jäger and Fratzl 2000] I. Jäger and P. Fratzl, “Mineralized collagen fibrils: a mechanical model with a staggered arrangement of mineral particles”, *Biophys. J.* **79**:4 (2000), 1737–1746.
- [Lakes 1993] R. Lakes, “Materials with structural hierarchy”, *Nature* **361**:6412 (1993), 511–515.
- [Liu et al. 2006] B. Liu, L. Zhang, and H. Gao, “Poisson ratio can play a crucial role in mechanical properties of biocomposites”, *Mech. Mater.* **38**:12 (2006), 1128–1142.
- [Liu et al. 2009] B. Liu, X. Feng, and S.-M. Zhang, “The effective Young’s modulus of composites beyond the Voigt estimation due to the Poisson effect”, *Compos. Sci. Technol.* **69**:13 (2009), 2198–2204.
- [Nemat-Nasser and Hori 1993] S. Nemat-Nasser and M. Hori, *Micromechanics: overall properties of heterogeneous materials*, North-Holland Series in Applied Mathematics and Mechanics **37**, Elsevier, Amsterdam, 1993.
- [Oshmyan et al. 2001] V. G. Oshmyan, S. A. Patlazhan, and S. A. Timan, “Elastic properties of Sierpinski-like carpets: finite element based formulation”, *Phys. Rev. E* **64**:5 (2001), Article ID #056108.
- [Picu and Soare 2009] R. C. Picu and M. A. Soare, “Mechanics of materials with self-similar hierarchical microstructure”, pp. 295–332 in *Multiscale modeling in solid mechanics: computational approaches*, edited by U. Galvanetto and M. H. F. Aliabadi, Imperial College Press, London, 2009.
- [Poutet et al. 1996] J. Poutet, D. Manzoni, F. Hage-Chehade, C. J. Jacquin, M. J. Bouteca, J.-F. Thovert, and P. M. Adler, “The effective mechanical properties of random porous media”, *J. Mech. Phys. Solids* **44**:10 (1996), 1587–1620.
- [Puxkandl et al. 2002] R. Puxkandl, I. Zizak, O. Paris, J. Keckes, W. Tesch, S. Bernstorff, P. Purslow, and P. Fratzl, “Viscoelastic properties of collagen: synchrotron radiation investigations and structural model”, *Phil. Trans. R. Soc. B* **357**:1418 (2002), 191–197.
- [Reuss 1929] A. Reuss, “Berechnung der Fließgrenze von Mischkristallen auf Grund der Plastizitätsbedingung für Einkristalle”, *Z. Angew. Math. Mech.* **9**:1 (1929), 49–58.
- [Sánchez-Palencia 1980] E. Sánchez-Palencia, *Non-homogeneous media and vibration theory*, Lecture Notes in Physics **127**, Springer, Berlin, 1980.
- [Steven 1997] G. P. Steven, “Homogenization of multicomponent orthotropic materials using FEA”, *Commun. Numer. Methods Eng.* **13**:7 (1997), 517–531.
- [Stratasys 2012] “Objet350 Connex multi-material 3D printer”, Stratasys, Eden Prairie, MN, 2012, <http://www.stratasys.com/3d-printers/design-series/precision/objet-connex350>.
- [Tan et al. 1999] P. Tan, L. Tong, and G. P. Steven, “Micromechanics models for the elastic constants and failure strengths of plain weave composites”, *Compos. Struct.* **47**:1–4 (1999), 797–804.
- [Tan et al. 2000] P. Tan, L. Tong, and G. P. Steven, “Behavior of 3D orthogonal woven CFRP composites, II: FEA and analytical modeling approaches”, *Compos. A Appl. Sci. Manuf.* **31**:3 (2000), 273–281.
- [Thovert et al. 1990] J. F. Thovert, F. Wary, and P. M. Adler, “Thermal conductivity of random media and regular fractals”, *J. Appl. Phys.* **68** (1990), 3872–3883.

- [Voigt 1889] W. Voigt, “Ueber die Beziehung zwischen den beiden Elasticitätsconstanten isotroper Körper”, *Ann. Physik* **274**:12 (1889), 573–587.
- [Watt et al. 1976] J. P. Watt, G. F. Davies, and R. J. O’Connell, “The elastic properties of composite materials”, *Rev. Geophys.* **14**:4 (1976), 541–563.
- [Xie and Steven 1993] Y. M. Xie and G. P. Steven, “A simple evolutionary procedure for structural optimization”, *Comput. Struct.* **49**:5 (1993), 885–896.
- [Xie and Steven 1997] Y. M. Xie and G. P. Steven, *Evolutionary structural optimization*, Springer, London, 1997.
- [Yang et al. 2013] X. Y. Yang, X. Huang, J. H. Rong, and Y. M. Xie, “Design of 3D orthotropic materials with prescribed ratios for effective Young’s moduli”, *Comput. Mater. Sci.* **67** (2013), 229–237.
- [Zhang et al. 2011] Z. Zhang, Y.-W. Zhang, and H. Gao, “On optimal hierarchy of load-bearing biological materials”, *Proc. R. Soc. Lond. B* **278**:1705 (2011), 519–525.

Received 27 Dec 2012. Revised 20 May 2013. Accepted 25 Jun 2013.

YI MIN XIE: [mike.xie@rmit.edu.au](mailto:mike.xie@rmit.edu.au)

Centre for Innovative Structures and Materials, School of Civil, Environmental and Chemical Engineering, RMIT University, GPO Box 2476, Melbourne VIC 3001, Australia

ZHI HAO ZUO: [zhihao.zuo@rmit.edu.au](mailto:zhihao.zuo@rmit.edu.au)

Centre for Innovative Structures and Materials, School of Civil, Environmental and Chemical Engineering, RMIT University, GPO Box 2476, Melbourne VIC 3001, Australia

XIAODONG HUANG: [huang.xiaodong@rmit.edu.au](mailto:huang.xiaodong@rmit.edu.au)

Centre for Innovative Structures and Materials, School of Civil, Environmental and Chemical Engineering, RMIT University, GPO Box 2476, Melbourne VIC 3001, Australia

XIAOYING YANG: [xiaoying.yang@rmit.edu.au](mailto:xiaoying.yang@rmit.edu.au)

Centre for Innovative Structures and Materials, School of Civil, Environmental and Chemical Engineering, RMIT University, GPO Box 2476, Melbourne VIC 3001, Australia

# JOURNAL OF MECHANICS OF MATERIALS AND STRUCTURES

[msp.org/jomms](http://msp.org/jomms)

Founded by Charles R. Steele and Marie-Louise Steele

## EDITORIAL BOARD

ADAIR R. AGUIAR University of São Paulo at São Carlos, Brazil  
KATIA BERTOLDI Harvard University, USA  
DAVIDE BIGONI University of Trento, Italy  
IWONA JASLUK University of Illinois at Urbana-Champaign, USA  
THOMAS J. PENCE Michigan State University, USA  
YASUhide SHINDO Tohoku University, Japan  
DAVID STEIGMANN University of California at Berkeley

## ADVISORY BOARD

J. P. CARTER University of Sydney, Australia  
R. M. CHRISTENSEN Stanford University, USA  
G. M. L. GLADWELL University of Waterloo, Canada  
D. H. HODGES Georgia Institute of Technology, USA  
J. HUTCHINSON Harvard University, USA  
C. HWU National Cheng Kung University, Taiwan  
B. L. KARIHALOO University of Wales, UK  
Y. Y. KIM Seoul National University, Republic of Korea  
Z. MROZ Academy of Science, Poland  
D. PAMPLONA Universidade Católica do Rio de Janeiro, Brazil  
M. B. RUBIN Technion, Haifa, Israel  
A. N. SHUPIKOV Ukrainian Academy of Sciences, Ukraine  
T. TARNAI University Budapest, Hungary  
F. Y. M. WAN University of California, Irvine, USA  
P. WRIGGERS Universität Hannover, Germany  
W. YANG Tsinghua University, China  
F. ZIEGLER Technische Universität Wien, Austria

**PRODUCTION** [production@msp.org](mailto:production@msp.org)

SILVIO LEVY Scientific Editor

Cover photo: Wikimedia Commons

---

See [msp.org/jomms](http://msp.org/jomms) for submission guidelines.


---

JoMMS (ISSN 1559-3959) at Mathematical Sciences Publishers, 798 Evans Hall #6840, c/o University of California, Berkeley, CA 94720-3840, is published in 10 issues a year. The subscription price for 2013 is US\$555/year for the electronic version, and \$705/year (+\$60, if shipping outside the US) for print and electronic. Subscriptions, requests for back issues, and changes of address should be sent to MSP.

---

JoMMS peer-review and production is managed by EditFLOW<sup>®</sup> from Mathematical Sciences Publishers.

PUBLISHED BY

 **mathematical sciences publishers**  
nonprofit scientific publishing

<http://msp.org/>

© 2013 Mathematical Sciences Publishers

- Efficiencies of algorithms for vibration-based delamination detection: A comparative study**                      **OBINNA K. IHESIULOR, KRISHNA SHANKAR, ZHIFANG ZHANG and TAPABRATA RAY**                      **247**
- Evaluation of the effective elastic moduli of particulate composites based on Maxwell's concept of equivalent inhomogeneity: microstructure-induced anisotropy**                      **VOLODYMYR I. KUSHCH, SOFIA G. MOGILEVSKAYA, HENRYK K. STOLARSKI and STEVEN L. CROUCH**                      **283**
- On successive differentiations of the rotation tensor: An application to nonlinear beam elements**                      **TEODORO MERLINI and MARCO MORANDINI**                      **305**
- Predicting the effective stiffness of cellular and composite materials with self-similar hierarchical microstructures**                      **YI MIN XIE, ZHI HAO ZUO, XIAODONG HUANG and XIAOYING YANG**                      **341**
- On acoustoelasticity and the elastic constants of soft biological tissues**                      **PHAM CHI VINH and JOSE MERODIO**                      **359**
- Identification of multilayered thin-film stress from nonlinear deformation of substrate**                      **KANG FU**                      **369**